

Heat and mass transfer analysis in air gap membrane distillation process for desalination

Bhauasaheb L. Pangarkar^{1*} and Mukund G. Sane²

¹Sir Visvesvaraya Institute of Technology, University of Pune, Chincholi, Nashik, 422 101, India

²National Chemical Laboratory, Pune, India

(Received April 21, 2011, Accepted July 11, 2011)

Abstract. The air gap membrane distillation (AGMD) process was applied for water desalination. The main objective of the present work was to study the heat and mass transfer mechanism of the process. The experiments were performed on a flat sheet module using aqueous NaCl solutions as a feed. The membrane employed was hydrophobic PTFE of pore size 0.22 μm . A mathematical model is proposed to evaluate the membrane mass transfer coefficient, thermal boundary layers' heat transfer coefficients, membrane / liquid interface temperatures and the temperature polarization coefficients. The mass transfer model was validated by the experimentally and fitted well with the combined Knudsen and molecular diffusion mechanism. The mass transfer coefficient increased with an increase in feed bulk temperature. The experimental parameters such as, feed temperature, 313 to 333 K, feed velocity, 0.8 to 1.8 m/s (turbulent flow region) were analyzed. The permeation fluxes increased with feed temperature and velocity. The effect of feed bulk temperature on the boundary layers' heat transfer coefficients was shown and fairly discussed. The temperature polarization coefficient increased with feed velocity and decreased with temperature. The values obtained were 0.56 to 0.82, indicating the effective heat transfer of the system. The fouling was observed during the 90 h experimental run in the application of natural ground water and seawater. The time dependent fouling resistance can be added in the total transport resistance.

Keywords: AGMD; desalination; heat transfer coefficient; mass transfer coefficient; temperature polarization coefficient

1. Introduction

Membrane distillation (MD) is a hybrid of thermal distillation and membrane separation process. The possible application of MD for desalination has been examined by some researchers (Pinappu 2010, Meindersma *et al.* 2006, Mohammadi *et al.* 2009, Mohammadali *et al.* 2009, Gryta 2010(a)). MD offers various advantages in comparison to the traditional distillation and pressure driven membrane processes (Tang *et al.* 2010). MD for water desalination is a membrane technique for separating water vapor from a liquid saline aqueous solution by transporting through the pores of hydrophobic membranes, made mainly of polypropylene (PP), polytetrafluoroethylene (PTFE), polyvinylidene fluoride (PVDF) and polyethylene (PE). Various types of methods may be employed to impose a vapor pressure difference across the membrane to drive a flux. The permeate side may be a cold liquid in direct contact with the membrane, called direct contact membrane distillation (DCMD) or a condensing surface separated from the membrane by an air gap called air gap membrane distillation (AGMD)

* Corresponding author, Assistant Professor, E-mail: pbl_1978@yahoo.com

or a sweep gas blown across the membrane called sweep gas membrane distillation (SGMD) or vacuumed called vacuum membrane distillation (VMD). Because AGMD and DCMD do not need an external condenser, they are best suited for applications where water is the permeating flux. (Tang *et al.* 2010, Izquierdo-Gil *et al.* 2003, Suk *et al.* 2010, Gryta 2010(b)).

In AGMD process, only the feed solution is in direct contact with the membrane. The permeate is condensed on a cold surface. There is an air gap situated between the membrane and the cold surface to reduce energy losses by heat conduction through the membrane as compared to other MD configurations. The main drawback of the air gap is that it is also an additional resistance to mass transfer. Air gap MD is suitable for all direct contact MD applications. However, it is also suitable to separate other volatile substances such as alcohols from an aqueous solution. In AGMD process, the permeate is not direct contact with the membrane, there is no danger of membrane wetting at the permeate side (Meindersma *et al.* 2006, Matheswaran *et al.* 2007).

In MD both heat and mass transfer from the feed side, across the boundary layer and membrane, to the permeate side. Large quantity of heat is used to vaporize the volatile component at the membrane surface. It results in the difference in temperature between bulk solution and membrane surface called as temperature polarization, and may cause a significant loss in the driving force of the process. Similarly, concentration polarization or mass transfer in boundary layer is taken into account in a high concentration system. It is contributed by the accumulation of non-volatile component at membrane surface, and results in the reduction of the imposed driving force and so the mass flux. However, concentration polarization generally has only little effect on the driving forces, and is always neglected (Srisurichan *et al.* 2006). Hence, this study intends to illustrate the details of all heat and mass transfer mechanisms based on the direct experimental observation of heat and mass fluxes. The performance of AGMD for desalination of ground water and seawater was investigated experimentally by using flat PTFE membrane and determining the optimal operating conditions, and to study the fouling phenomena.

2. Theory

MD technology took more academic role and most of the publications in MD field are concerned with experimental studies on the effects of the process operating conditions and theoretical models including heat and mass transfer mechanisms. However, MD technology is still not fully developed at industrial scale, although it has been known for more than forty years and used successfully in numerous applications such as in desalination. A more intensive and focused research efforts in MD are needed, both in experimental and modeling, where the central issues are the high energy consumption in MD units, heat recovery, difficulties with long term operations with risk of membrane pores wetting and membrane fouling and lack of MD membranes and module designed for this process.

Transport of gases and vapors through porous media has been extensively studied and theoretical models have been developed based on the kinetic theory of gases to predict the MD performance of the membranes depending on the MD configuration used (Meindersma *et al.* 2006, Khayet 2010, Deshmukh *et al.* 2010, Qtaishat *et al.* 2008, Termpiyakua *et al.* 2005, Khayet *et al.* 2010, Lawson *et al.* 1996, Imdakma *et al.* 2007, Close *et al.* 2010). Different types of mechanisms proposed for the mass transport are: Knudsen flow model, viscous flow model, molecular diffusion model and /or combination between them. In general, mass transfer in MD occurs by convective and diffusive transport of volatile species through the membrane pores. Molecular diffusion has a partial pressure

difference as driving force and non-identical molecules that are in the way form the resistance to mass transfer. The driving force for Knudsen diffusion is also a partial pressure difference, but in this case molecules bounce into the membrane matrix, which forms the resistance mass transfer. Knudsen diffusion is thus important for small pores and /or low pressure. Finally, viscous flow has a water vapor pressure difference as driving force, and the membrane matrix forms the resistance against it (Meindersma *et al.* 2006, Khayet 2010, Qtaishat *et al.* 2008, Banat *et al.* 2003, Baon *et al.* 2005).

The governing quantity which provides a guideline in determining the operative mechanism in a given membrane pore under a given experimental condition is Knudsen number (k_n) defined (Eq. (1)) as the ratio of mean free path, λ , and pore diameter, d_p .

$$k_n = \frac{\lambda}{d_p} \quad (1)$$

The mean free path, λ , can be calculated by the following expression as

$$\lambda = \frac{3.2 \mu_v}{p} \sqrt{\frac{RT}{2\pi M}} \quad (2)$$

Where, μ_v is viscosity of vapors at atmospheric temperature and ambient pressure, M is molecular weight, R is gas constant, T is temperature, P is the mean pressure within the pores.

If k_n is less than 0.01, the mass transfer mechanism is considered as molecular diffusion and k_n values higher than 10, the mechanism is considered as Knudsen diffusion. If the value of k_n lies between 0.01 to 10, it is the transition zone and both the mechanism contributes to the mass transfer (Deshmukh *et al.* 2010, Imdakma *et al.* 2007, Lawson *et al.* 1996).

The following set of equations has been considered in MD for different mass transport mechanisms.

$$\frac{j_i^D}{D_{i,e}^k} + \frac{P j_i^D - P j_j^D}{D_{i,j,e}^D} = -\frac{1}{RT} \nabla p_i \quad (3)$$

$$j_i^v = -\frac{\varepsilon d_p^2 p_i}{32RT\tau\mu} \nabla p_i \quad (4)$$

$$j_i = j_i^v + j_i^D \quad (5)$$

$$D_{i,e}^k = \frac{\varepsilon d_p}{3\tau} \sqrt{\frac{8RT}{\pi M}} \quad (6)$$

$$D_e = \frac{\varepsilon P D}{\tau} \quad (7)$$

Where, j^D is the diffusive type of flux, j^v is the viscous type of flux, D^k is the Knudsen diffusion coefficient, D is the molecular diffusion coefficient, P is the total pressure, ε is the membrane porosity, τ is the pore tortuosity, and the subscripts e refers to the effective, i for water and j for air.

The membrane permeates flux, j_i , which is dependent on the membrane characteristics and the established driving force can be expressed as (Meindersma *et al.* 2006, Khayet 2010).

$$j_i = B_i \Delta p_i \quad (8)$$

Where, B_i is the membrane distillation coefficient of the membrane, Δp_i is the water vapor

pressure difference between evaporating and condensing surface. The vapor pressure of the pure water component determined with the Antoine equation.

$$p_i = \exp\left[23.1964 - \frac{3816.44}{T - 46.13}\right] \quad (9)$$

In AGMD configuration, transport of vapor across the membrane was assumed to be considered by the theory of molecular diffusion admitting as a stagnant film, the air inside the pores of the membrane and in the space between the membrane and the condensing surface in the permeate side of the membrane module. The low solubility of air in water and the negligible air flux through the membrane permit to establish a pressure gradient apposite to the water vapor flux. Therefore, air can be treated a stagnant film and the expression for steady state diffusion of water vapor through a stagnant film were written as (Banat *et al.* 1998)

$$B_i^D = \frac{M_i \varepsilon PD}{RT \tau \delta p_a} \quad (10)$$

Where, p_a is the mean air pressure, δ is the membrane thickness, and B_i^D is the mass transfer coefficient for molecular diffusion mechanism.

The mass flux can be written for AGMD process in terms of pressure as (Banat *et al.* 1998, 1999)

$$j_i = \frac{DP}{RTb|Pa|_{lm}} \Delta p_i \quad (11)$$

Where, b is the air gap thickness and $|Pa|_{lm}$ is the log mean of the air pressure at both sides of the membrane defined as

$$|Pa|_{lm} = \frac{P_{a1} - P_{a2}}{\ln \frac{P_{a1}}{P_{a2}}} \quad (12)$$

To account for the membrane porosity, thickness and tortuosity, the effective molar flux was expressed as

$$j_i = \frac{\varepsilon DP}{RT(\delta \tau + b)|Pa|_{lm}} \Delta p_i \quad (13)$$

If the vapor flux is controlled by diffusion through the membrane pores and natural convection through the air gap, the final derivation of the mass flux is expressed as (Chang *et al.* 2011, Bouguecha *et al.* 2002)

$$j_i = \frac{B_{i,T}}{RT} \Delta p_i \quad (14)$$

Where, $B_{i,T}$ is the overall membrane mass transfer coefficient. If $B_{i,cav}$ is the convective mass transfer coefficient in the air gap and $B_{i,D}$ is the diffusive mass transfer coefficient through the membrane.

$$B_{i,T} = \frac{1}{\frac{1}{B_{i,D}} + \frac{1}{B_{i,cav}}} \quad (15)$$

The membrane mass transfer coefficient of Knudsen diffusion mechanism (B_i^k) is calculated by the Eq. (16) as

$$B_i^k = \frac{2 \varepsilon r}{3 \tau \delta} \left(\frac{8 M_i}{\pi R T} \right)^2 \quad (16)$$

The mass transfer coefficient of combined (Knudsen and molecular diffusion) mechanism (B_i^c) is calculated by the Eq. (17) as

$$B_i^c = \left[\frac{3 \tau \delta}{2 \varepsilon r} \left(\frac{\pi R T}{8 M_i} \right)^{1/2} + \frac{\tau \delta p_a R T}{\varepsilon P D M} \right]^{-1} \quad (17)$$

And

$$P D = 1.895 \times 10^{-5} T^{2.072} \quad (18)$$

In MD, a coupled heat and mass transfer occurs an enthalpy flux exists across the hydrophobic membrane from the feed to permeate. The detailed mechanism of heat and mass transfer and temperature profile in AGMD process is shown in Fig. 1. The heat transport can be described by three steps: i) heat transport through feed boundary layer, ii) heat transport through the membrane, and iii) heat transport through the permeate boundary layer. The total heat flux through the membrane, Q_m , is due to two mechanisms: -i) conduction across the membrane material and its gas filled pores (Q_c) and -ii) latent heat associated to the vaporized molecules (Q_v). Therefore the equation written as

$$Q_m = Q_c + Q_v = -k_m \frac{dT}{dx} + j_i \Delta H_{v,i} \quad (19)$$

Where, $\Delta H_{v,i}$ is the evaporation enthalpy of species i at the absolute temperature, T , of the transmembrane flux, J_i , k_m is the thermal conductivity of the membrane and x is the distance across the membrane. The Eq. (19) can be written as

$$Q_m = k_m (T_{m1} - T_{m2}) + j_i \Delta H_{v,i} \quad (20)$$

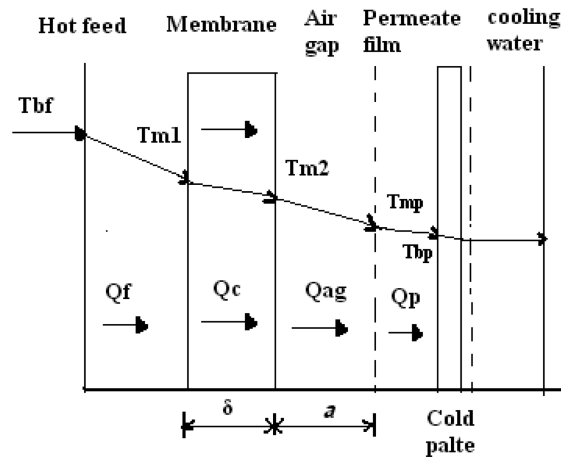


Fig. 1. Temperature profile, and Heat and mass transfer mechanism in AGMD.

Where, T_{m1} and T_{m2} are the temperature at feed side and permeate side membrane surface respectively. Various models have been considered to calculate the thermal conductivity of the MD membrane. In general the following expression has been used (Celere *et al.* 2002)

$$k_m = \varepsilon k_g + (1 - \varepsilon)k_p \quad (21)$$

Where, k_p is the thermal conductivity of the membrane matrix and k_g is the thermal conductivity of the gas. The heat transfer coefficient of the membrane can be written as

$$h_m = \frac{k_m}{\delta} \quad (22)$$

Where, h_m is the heat transfer coefficient of membrane. The total heat flux in the air gap (Q_{ag}) can be written as

$$Q_{ag} = h_{ag}(T_{m2} - T_{mp1}) + j_i \Delta H_{v,i} \quad (23)$$

Where, h_{ag} is the heat transfer coefficient in air gap and T_{mp1} is the temperature at the permeate boundary layer. If k_{ag} is the thermal conductivity of the air and a is the air gap thickness, then the heat transfer coefficient of air gap can be calculated as

$$h_{ag} = \frac{k_{ag}}{a} \quad (24)$$

Hence the total heat flux can be calculated as

$$Q = \left[\frac{1}{h_f} + \frac{1}{\frac{k_m}{\delta} + j_i \Delta H_{v,i} / \Delta T_m} + \frac{1}{h_{ag}} + \frac{1}{h_p} \right]^{-1} \Delta T = H \Delta T \quad (25)$$

Where, ΔT is the bulk temperature difference between feed and permeate ($T_{b,f} - T_{b,p}$) and ΔT_m is the transmembrane temperature difference ($T_{m1} - T_{m2}$), h_f and h_p are the heat transfer coefficient in the feed and permeate boundary layers respectively, H is the global heat transfer coefficient of the MD process.

The temperature polarization coefficient (θ) is generally used as an indirect coefficient to quantify the magnitude of the boundary layer resistance over the total heat transfer resistance. It is defined as

$$\theta = \frac{T_{m1} - T_{m2}}{T_{b,f} - T_{b,p}} \quad (26)$$

For well designed MD modules, the θ approaches to unity. However, for MD modules with high thermal boundary layer resistances, θ values are very low; the MD process is heat transfer limited. An enhancement of the θ with the increase of both the feed and permeate flow rates, with a decrease of the temperature, especially the feed temperature, and it is strongly dependant on membrane characteristics (Khayet 2010, Termpiyakua *et al.* 2005, Bouguecha *et al.* 2002, Celere *et al.* 2002, Charfi *et al.* 2010).

The interfacial temperatures T_{m1} and T_{m2} at feed side and permeate side respectively cannot be measured directly. However, they were estimated from the energy balance equation at steady state conditions. The interfacial temperatures can be written as

$$T_{m1} = \frac{k_m/\delta \left[T_{bp} + \frac{h_f}{h_p} T_{bf} \right] + h_f T_{bf} - j_i \Delta H_{v,i}}{\frac{k_m}{\delta} + h_f \left[1 + \frac{k_m}{\delta h_p} \right]} \quad (27)$$

And

$$T_{m2} = \frac{k_m/\delta \left[T_{bf} + \frac{h_p}{h_f} T_{bp} \right] + h_p T_{bp} - j_i \Delta H_{v,i}}{\frac{k_m}{\delta} + h_p \left[1 + \frac{k_m}{\delta h_f} \right]} \quad (28)$$

The following correlations are generally used in MD for estimation of the boundary layers heat transfer coefficients, h_f and h_p as (Banat *et al.* 1999(b), Martinez-Diez *et al.* 1999, Mengual *et al.* 2004, Schofield *et al.* 1987, Martinez-Diez *et al.* 1996)

When $Re < \approx 2100$ (Laminar flow)

$$Nu = 1.86(RePr d_h/L)^{1/3} \quad (29)$$

When $2000 \approx < Re < \approx 6000$ (Transitional flow)

$$Nu = 0.116(Re^{2/3} - 125)Pr^{1/3} \left[1 + \left(\frac{d_h}{L} \right)^{2/3} \right] \quad (30)$$

When $Re > \approx 6000$ (Turbulent flow)

$$Nu = 0.023Re^{4/5}Pr^m \quad (31)$$

Where, L is the channel length, d_h is the hydraulic diameter, Re is the Reynolds number, Pr is the Prandtl number, Nu is the Nusselt number.

The similarities between the governing equations for heat and mass transfer suggest that empirical correlations for the mass transfer coefficient would be similar to those for the heat transfer coefficients may be related to the Reynolds analogy yielding to the mass transfer coefficient is known (Bouguecha *et al.* 2002).

3. Experimental

The experimental process simply consists of a flat sheet hydrophobic micro porous PTFE membrane (Millipore) fixed in the PVC pipe, feed compartment (150 × 25 mm) and cooling compartment (150 × 25 mm) as shown in Fig. 2. The effective area of the membrane was 3.6 cm², membrane thickness, 175 μm, pore size, 0.22 μm and porosity, 70%. The permeate vapor diffused through the membrane and condensed due to contact with the cooling plate. The cold water was used as a coolant in the cooling compartment. The permeated liquid was collected in a graduated cylinder and the volume of permeate collected was noted with regular intervals of time and the collected samples were analyzed simultaneously. The inlet temperature of the hot feed and coolant were maintained constant throughout the experiment. The two types of aqueous feed solution such as lower concentration, 5 g/l and higher concentration, 20 g/l NaCl in pure water were prepared and continuously fed to the membrane module

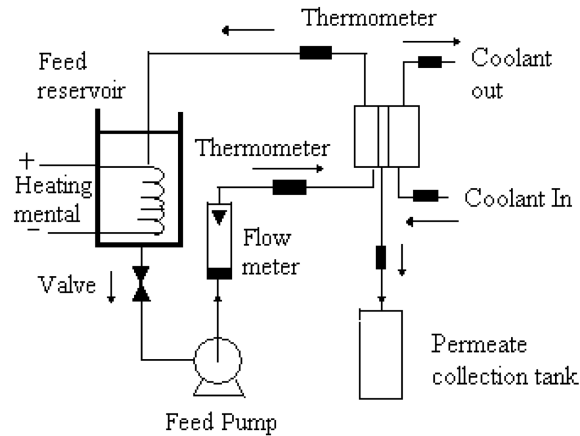


Fig. 2. AGMD experimental setup.

from a reservoir by using a pump. All the AGMD experiments were carried out for 3-4 h and after almost 3 h; the flux reaches steady state or equilibrium.

4. Results and discussions

4.1 Effect of temperature

It is well known that in MD processes, temperature is the operating variable that affects the MD flux most significantly due to the exponential increase of vapor pressure with temperature, as already proved by a number of studies [Qtaishat *et al.* 2008, Termpiyakua *et al.* 2005, Lawson *et al.* 1996, Banat *et al.* 2003]. Fig. 3 is showing the effect of feed temperature on permeation flux at feed flow rate, 55 l/h, coolant temperature, 288 K, and air gap thickness, 1.2 mm for the commercial PTFE membrane. The permeate flux increased with increasing feed temperature from 313 K to 333 K. The permeation flux was reached 22.45 kg/m²h for 5 g/l salt solution and 19.87 kg/m²h for 20 g/l

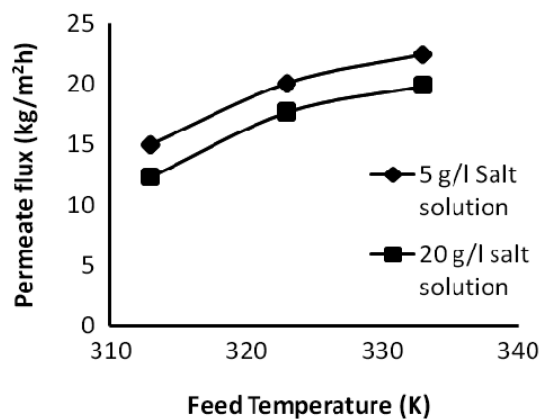


Fig. 3. Effect of feed temperature at feed flow rate, 55 l/h, coolant temperature, 288 K.

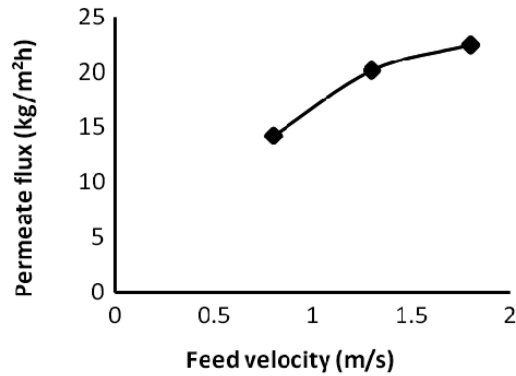


Fig. 4. Effect of feed velocity of feed salt concentration, 5 g/l, feed temperature, 333 K, coolant temperature, 288 K.

salt solution. It indicates that the flux decreases only slightly increasing feed salt concentration.

4.2 Effect of feed velocity

Fig. 4 depicts the flux- feed velocity curve at feed salt concentration 5 g/l, feed temperature, 333 K, coolant temperature, 288 K. The feed water velocity changes between 0.8 m/s and 1.8 m/s (turbulent flow). The efficient method for flux enhancement is to provide highly turbulent flow across both the membrane faces. This is achieved by driving feed and permeates streams at high flow rates. The formation of the temperature boundary layer is mainly brought about by the water vaporization on the membrane surface. At a given temperature, the Reynolds number increases with an increasing feed flow rate, which causes the enhanced mixing of the flow channels to develop the turbulence. Due to this, the temperature polarization coefficient and heat transfer coefficient increases. Hence, the vapor transfer resistance through the membrane means membrane mass transfer resistance decreases and permeation flux increases. After 1.8 m/s feed velocity, no effect was found on the permeation flux for both feed water. Salt rejection was greater than 99.9 % throughout all the experiments.

4.3 Analysis of mass transfer coefficient

The mechanism of mass transfer in the membrane can be from the Knudsen number (k_n). Hence, from Eq. (1), k_n was approximately 0.54, and this falls in the transition region in which both Knudsen diffusion and molecular diffusion play an important role. The mass transfer coefficient, of the membrane was calculated by experimentally (by Eq. (8)) and theoretically (by Eq. (17)) at different feed bulk temperatures as shown in Fig. 5 for aqueous NaCl solution of 5 g/l concentration. Generally, the mass transfer coefficient increases with an increase in the feed bulk temperature. Since increasing the feed bulk temperature will lead to an increase in the water vapor diffusion coefficient through stagnant air. Moreover, the water vapor flux increases as the feed temperature increased as shown in Fig. 3. Both experimental and theoretical values are of the same order and magnitude. Some deviations of the experimental values from theoretical ones are shown in Fig. 5.

For comparison, the membrane mass transfer coefficient was also calculated for the aqueous salt feed of 20 g/l and was found to be 3.1×10^{-3} kg/m²h.Pa. The difference was approximately 11%. Therefore, the mass transfer coefficient obtained from lower salt feed solution may be used for flux prediction except at high feed concentrations.

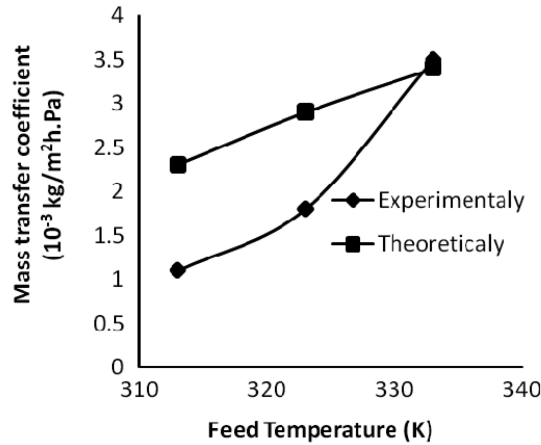


Fig. 5. Effect of feed bulk temperature on mass transfer coefficient.

4.4 Effect of boundary layer heat transfer coefficient

There is a variety of empirical correlations that can be used to estimate the boundary layer's heat transfer coefficients. Eq. (31) was chosen in our model development due to the assumption of turbulent flow inside the membrane module. The feed side boundary layer heat transfer coefficient, h_f and permeate side heat transfer coefficient, h_p were calculated with different average membrane temperature, T_m , by using the heat transfer correlations. The effects are shown in Fig. 6. As can be seen, the heat transfers coefficients of both feed and permeate vary with temperature of membrane. The heat transfer coefficients in the feed side of membrane is higher than in the permeate side. This is due to the fact that the feed temperature is higher than the permeate temperature affecting the hydrodynamics parameters of the feed and permeate liquid. The heat transfer coefficient increased by 27% on the feed side, while it was only 0.6% on the permeate side with a T_m increases from 310.5 to 314.5 K. This is because the variation of the temperature on the feed side was more significant than on the permeate side.

The MD flux increases with the feed flow rate because of increased Re and decreased boundary layer resistances. At higher Re, high heat transfer from the bulk feed to the membrane surface approaches to the corresponding temperature in the bulk phases leading to greater MD flux and

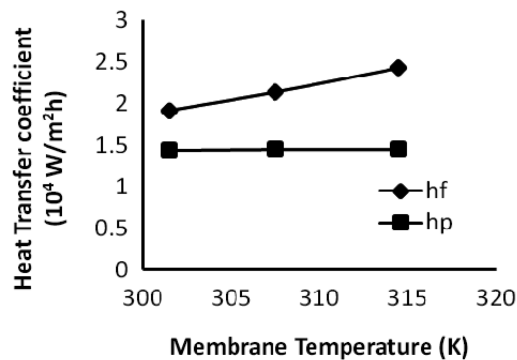


Fig. 6. Effect of membrane temperature on boundary layers heat transfer coefficients.

corresponding increase in the heat transfer coefficient. As the heat transfer coefficient increases, the temperature at the membrane surface approaches to the bulk temperature and the vapor pressure driving force increases.

4.5 Temperature polarization effect

To illustrate the temperature polarization of the system, the coefficients (θ) are presented in Figs. 7 and 8. The increase of feed velocity resulted in higher θ . On other hand, the coefficient decreased with feed bulk temperature. An increase in feed bulk temperature leads to an increase in the energy consumed by vaporization of water at the higher temperatures. As a result, the temperature polarization effect will be more significant, or in θ will be lower. Generally, for satisfactory MD modules, θ values ranges between 0.4 and 0.7 (Khayet, 2010, Qtaishat, *et al.* 2008). The θ values ranges between 0.56 and 0.82 indicating the appropriate design of the system. It was also observed an enhancement of the θ with the increase of both feed and permeates flow rates and it is strongly dependant on membrane characteristics. The produced high values of θ are due to the high values of the boundary layers heat transfer coefficients, which reflect the high feed and permeate flow rates and the flow turbulence. This further leads to a significant decrease in the temperature polarization effect due to the decrease in the thermal boundary layers' resistances (Qtaishat, *et al.* 2008).

4.6 Fouling and mass transfer resistances

Fouling and scaling are two important mechanisms that affect stability of MD process and lead to reduce the overall performance. Deposit reports that membrane fouling in MD is less problematic than in other processes due to large pore size, the phenomena is not studied, either experimentally or analytically (Kullab, *et al.* 2011). In AGMD process, the total resistance without the presence of fouling layer is composed of the resistance in feed boundary layer (R_{fb}), resistance of membrane (R_m), resistance in air gap (R_{ag}), and the resistance in permeate boundary layer (R_{pb}) (see Fig. 1). In these transport resistances, the feed boundary layer played important role in MD process. The effects of feed velocity and feed temperature on the feed boundary layer are seen in the section 4.1 and 4.2.

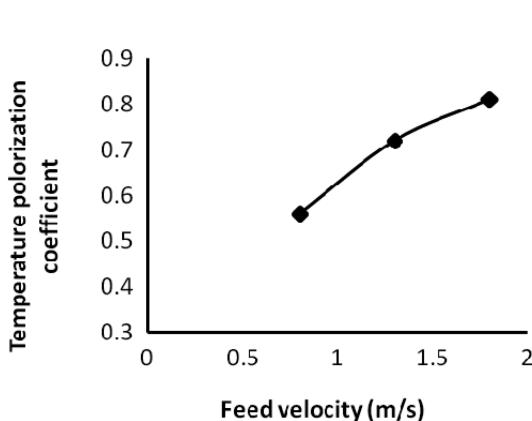


Fig. 7. Effect of feed velocity on temperature polarization coefficient.

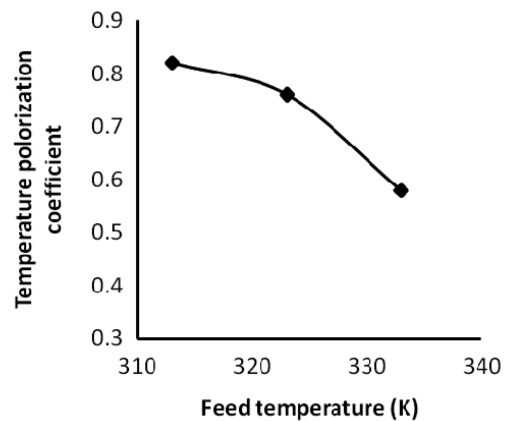


Fig. 8. Effect of feed temperature on temperature polarization coefficient.

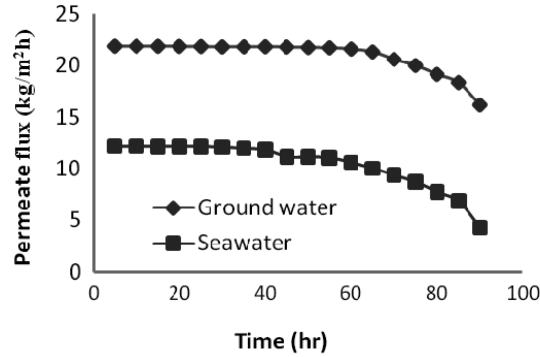


Fig. 9. Time variation of permeate flux of natural ground water and seawater at feed flow rate, 55 l/h, feed temperature, 333 K and coolant temperature, 288 K.

The application of AGMD on the natural ground water and seawater were performed with the feed flow rate, 55 l/h; feed temperature, 333 K; coolant temperature 288 K; air gap thickness, 1.2 mm. The experimental results of long term experimentation shown in Fig. 9 demonstrate that the direct application of the natural ground water and seawater as a feed for AGMD process resulted in a rapid decline of the permeate flux. This is due to the formation of the deposits on the membrane surface. This scale deposits scattered on the membrane surface would cause pores clogging and pollute the membrane. Therefore, the permeate flux was decreased with the prolongation of operating time. Although the scale deposits polluted with the membrane, the quality of obtained permeate was maintained. The initial flux of 21.87 kg/m²h which was decline to 16.93 kg/m²h for ground water and 12.11 kg/m²h to 4.89 kg/m²h for seawater over 90 h continuously at constant operating conditions. The flux decreases represents 23% for ground water and 60% for seawater, in 90 h. The permeate flux was nearly constant up to 65 h for ground water and up to 40 h for seawater and after that the flux decline rapidly, means the scale deposits start after 65 h for ground water feed and after 40 h for seawater feed. Due to the higher concentrations of the species in seawater, the deposits on the membrane surface is higher as compared to the ground water.

Hence in AGMD process, the fouling was observed due to the formation of a cake layer on the membrane surface. The particles deposit onto the membrane surface in the cake form, and the change of total resistance due to the resistance of cake layer. With the formation of a cake layer, the time dependent fouling resistance ($R_f(t)$) can be added into the total resistance as follows

$$R_t(t) = R_{fb} + R_f(t) + R_m + R_{ag} + R_{pb} \quad (32)$$

In order to eliminate the negative effect of scale deposition on the membrane surface, AGMD process were carried out at the initial feed pH 4 adjusted by addition of 0.1 mol/l HCl to the feed. The results of Fig. 10 was seen, the acidification of the feed enhances the stability of the process in a significant degree. There was negligible (<14%) decline of permeate flux for ground water and seawater during 180 h continuous operating process. Hence, addition of HCl in water (acidification of feed) was an efficient method to eliminate the negative effect of scale deposits on the surface of the membrane. Therefore, the membrane resistance was unaffected because there was no particle deposition within the pores.

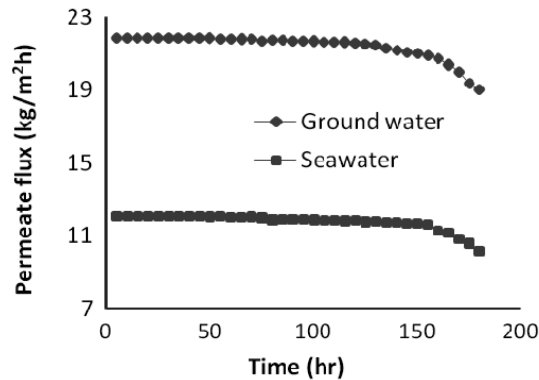


Fig. 10. Time variation of permeate flux with maintaining initial pH 4 by adjusting 0.1 mol/l HCl to the feed.

5. Conclusions

An experimental study of AGMD process was reported for desalination of low and high saline water by using a flat sheet membrane module configuration. The membrane mass transfer coefficient obtained from 5 g/l salt water feed and agreed with the theoretical mass transfer coefficient. The combined (Knudsen and molecular diffusion) model was validate for mass transfer. For comparison, the membrane mass transfer coefficient for high saline water was also calculated and found the difference approximately 11%. The effect of water feed velocity; feed bulk temperature on the MD flux has been discussed. The boundary layers' heat transfer coefficients and temperature polarization coefficient were estimated from the measurements of the permeate flux and the feed inlet and outlet temperatures. The boundary layers' heat transfer coefficients increases as the feed bulk temperature increased. The temperature polarization coefficient value increased with feed flow rate and decreased with feed bulk temperature in the range between 0.56 and 0.82. In the application of natural ground water and seawater, the membrane fouling was observed during 90 h experimental run. This fouling can be controlled by the acidification of the feed water, maintain the initial pH 4 adjusted by adding 0.1 mol/l HCl to feed water.

Acknowledgements

We are deeply indebted to University of Pune, Pune for the financial support for this research work and also especially thankful to Dr. S.G. Wakchaure for his constant support during the experimental work.

References

- Banat, F.A. and Simandl, J. (1998), "Desalination by membrane distillation: A parametric study", *Sep. Sci. and Tech.*, **33**, 201-226.
- Banat, F.A. and Simandl, J. (1999), "Membrane distillation for dilute methanol: separation from aqueous streams", *J. Membrane Sci.*, **163**(2), 333-348.

- Banat, F.A., Abu Al-Rub, A., Jumah, R. and Al-Shamag, M. (1999), "Modeling of desalination using tubular direct contact distillation modules", *Sep. Sci. and Tech.*, **34**, 2191-2206.
- Banat, F., Abu Al-Rub, F. and Khalid Bani-Melhem (2003), "Desalination by vacuum membrane distillation: sensitivity analysis", *Separation and Purification Technology*, **33**(1), 75-87.
- Li, B. and Kamallesh K. Sirkar (2005), "Novel membrane and device for vacuum membrane distillation- based desalination process", *J. Membrane Sci.*, **257**(1-2), 60-75.
- Bouguecha, S., Chouikh, R. and Dhahbi, M. (2002), "Numerical study of the coupled heat and mass transfer in membrane distillation", *Desalination*, **152**(1-3), 245-252.
- Celere, M. and Gostoli, C. (2002), "The heat and mass transfer phenomena in osmotic membrane distillation", *Desalination*, **147**(1-3), 133-138.
- Chang, H., Chang, C.L., Ho, C.D., Li, C.C. and Wang, P.H. (2011), "Experimental and simulation of an air gap membrane distillation module with solar absorption function for desalination", *Desalination and Water Treatment*, **25**, 251-258.
- Charfi, K., Khayet, M. and Safi, M.J. (2010), "Numerical simulation and experimental studies on heat and mass transfer using sweeping gas membrane distillation", *Desalination*, **259**(1-3), 84-96.
- Edward, C. and Eva, S. (2010), "Modeling of direct contact membrane distillation for desalination", *20th European symposium on computer aided process engineering*, **28**, 649-654.
- Deshmukh, S.K. and Tajane, M.M. (2010), "Performance enhancement of Membrane Distillation process in fruit juice concentration by membrane surface modification", *World Academy of Science, Engineering and Technology*, **72**, 265-270.
- Gryta M. (2010), "Desalination of thermally softened water by membrane distillation process", *Desalination*, **257**(1-3), 30-35.
- Gryta M. (2010), "Application of membrane distillation process for tap water purification", *Membrane Water Treatment*, **1**(1), 1-12.
- Imdakma, A.O., Khayet, M. and Matsuura, T. (2007), "A Monte Carlo simulation model for vacuum membrane distillation process", *J. Membrane Sci.*, **306**, 341-348.
- Izquierdo-Gil, M.A. and Jonsson, G. (2003), "Factors affecting flux and ethanol separation performance in vacuum membrane distillation", *J. Membrane Sci.*, **214**(1), 113-130.
- Khayet, M. (2010), "Membranes and theoretical modeling of membrane distillation: A review", *Advances in Colloid and Interface Science*, In press.
- Khayet, M., Imdakm, A.O. and Matsuura, T. (2010), "Monte Carlo simulation and experimental heat and mass transfer in direct contact membrane distillation", *Inter. J. Heat and Mass Transfer*, **53**(7-8), 1249-1259.
- Kullab, A. and Martin, A. (2011), "Membrane distillation and applications for water purification in thermal cogeneration plants", *Separation and Purification Technology*, **76**, 231-237.
- Lawson, K.W. and Lloyd, D.R. (1996), "Membrane distillation. I. Module design and performance evaluation using vacuum membrane distillation", *J. Membrane Sci.*, **120**(1), 111-121.
- Martinez-Diez, L. and Vazquez-Gonzalez, M.I. (1999), "Temperature and concentration polarization in membrane distillation of aqueous salt solutions", *J. Membrane Sci.*, **156**(2), 265-273.
- Martinez-Diez, L. and Vazquez-Gonzalez, M.I. (1996), "Temperature polarization in mass transport through hydrophobic porous membranes", *AIChE J.*, **42**(7), 1844-1852.
- Matheswaran, M., Kwon, T.O., Kim, J.W. and Moon, S. (2007), "Factors affecting flux and water separation performance in air gap membrane distillation", *J. Ind. Eng. Chem.*, **13**(6), 965-970.
- Meindersma, G.W., Guijt, C.M. and de Haan, A.B. (2006), "Desalination and water recycling by air gap membrane distillation", *Desalination*, **187**(1-3), 291-301.
- Mengual, J.I., Khayet, M. and Godino, M.P. (2004), "Heat and mass transfer in vacuum membrane distillation", *Inter. J. Heat and Mass Transf.*, **47**(4), 865-875.
- Mohammadi, T. and Mohammad, A.S. (2009), "Application of Taguchi method in optimization of desalination by vacuum membrane distillation", *Desalination*, **249**(1), 83-89.
- Mohammadali, S. and Mohammadi, T. (2009), "High -salinity water desalination using VMD", *Chem. Eng. J.*, **149**(1-3), 191-195.
- Pinappu Sai R (2010), "Composite membranes for membrane distillation desalination process", *Final report, New Mexico State University*.

- Qtaishat, M., Matsuura, T., Kruczek, B. and Khayet, M. (2008), "Heat and mass transfer analysis in direct contact membrane distillation", *Desalination*, **219**(1-3), 272-292.
- Schofield, R.W., Fane, A.G. and Fell, C.J.D. (1990), "Gas and vapor transport through micro porous membranes: II. Membrane Distillation", *J. Membrane Sci.*, **53**(1-2), 173-185.
- Schofield, R.W., Fane, A.G. and Fell, C.J.D. (1987), "Heat and mass transfer in membrane distillation", *J. Membrane Sci.*, **33**(3), 299-313.
- Srisurichan, S., Jiratananon, R. and Fane, A.G. (2006) "Mass transfer mechanisms and transport resistances in direct contact membrane distillation process", *J. Membrane Sci.*, **277**(1-2), 186-194.
- Suk, D.E., Matsuura, T., Park, H.B. and Lee, Y.M. (2010), "Development of novel surface modified phase inversion membranes having hydrophobic surface-modifying macromolecule for vacuum membrane distillation", *Desalination*, **261**(3), 300-312.
- Tang, N., Jia, Q., Zhang, H., Li, J. and Cao, S. (2010), "Preparation and morphological characterization of narrow pore size distributed polypropylene hydrophobic membranes for vacuum membrane distillation via thermally induced phase separation", *Desalination*, **256**(1-3), 27-36.
- Termpiyakua, P., Jiratananon, R. and Srisurichan, S. (2005), "Heat and mass transfer characteristics of a direct contact membrane distillation process for desalination", *Desalination*, **177**, 133-141.

RJ